ATES, M. and FERNANDEZ, C. 2019. Ruthenium oxide-carbon-based nanofiller-reinforced conducting polymer nanocomposites and their supercapacitor applications. *Polymer bulletin* [online], 76(5), pages 2601-2619. Available from: https://doi.org/10.1007/s00289-018-2492-x

Ruthenium oxide-carbon-based nanofiller-reinforced conducting polymer nanocomposites and their supercapacitor applications.

ATES, M., FERNANDEZ, C.

2019

Ruthenium oxide–carbon-based nanofiller-reinforced conducting polymer nanocomposites and their supercapacitor applications

Murat Ates[1] · **Carlos Fernandez**[2]

Received: 24 November 2017 / Revised: 24 June 2018 / Accepted: 20 August 2018

Abstract

In this review article, we have presented for the first time the new applications of supercapacitor technologies and working principles of the family of RuO_2–carbon-based nanofiller-reinforced conducting polymer nanocomposites. Our review focuses on pseudocapacitors and symmetric and asymmetric supercapacitors. Over the last years, the supercapacitors as a new technology in energy storage systems have attracted more and more attention. They have some unique characteristics such as fast charge/discharge capability, high energy and power densities, and long stability. However, the need for economic, compatible, and easy synthesis materials for supercapacitors have led to the development of RuO_2–carbon-based nanofiller-reinforced conducting polymer nanocomposites with RuO_2. Therefore, the aim of this manuscript was to review RuO_2–carbon-based nanofiller-reinforced conducting polymer nanocomposites with RuO_2 over the last 17 years.

Keywords RuO_2 nanosheet · Faradaic redox reactions · Pseudocapacitance · Asymmetric supercapacitors · Energy storage · Nanocomposite · Carbon materials · Conducting polymer

Abbreviations

AC	Active carbon
ACNF	Active carbon nanofibers
AQ	Antraquinone
CeO_2	Cerium oxide

✉ Murat Ates
mates@nku.edu.tr
http://mates.nku.edu.tr/
http://www.atespolymer.org

1 Physical Chemistry Division, Department of Chemistry, Faculty of Arts and Sciences, Namik Kemal University, Degirmenalti Campus, 59030 Tekirdag, Turkey

2 School of Pharmacy and Life Sciences, Robert Gordon University, Garthdee Road, Aberdeen AB107GJ, UK

CF	Carbon fiber
CNTs	Carbon nanotubes
Co_3O_4	Cobalt oxide
C_{sp}	Specific capacitance
CV	Cyclic voltammogram
CVD	Chemical vapor deposition
DAAQ	1-4-Diaminoantraquinone
EDLC	Electrochemical double-layer capacitance
EPD	Electrophoretic deposition
EQCN	Electrochemical quartz crystal nanobalance
GO	Graphene oxide
GN	Graphene
RuO_2	Ruthenium oxide
h-RuO_2	Hydrous ruthenium oxide
h-RuO_2/MWCNT	Hydrous ruthenium oxide/multi-walled carbon nanotube
HRGO	Holey reduced graphene oxide
MnO_2	Mangane(IV) oxide
NiO	Nickel(II) oxide
PAN	Polyacrylonitrile
PANI	Polyaniline
PEDOT	Poly(3,4-ethylenedioxythiophene)
PEG	Polyethylene glycol
PEO	Polyethylene oxide
PCL	Poly(epsilon-caprolactone)
PCM	Phase change materials
PVA	Polyvinyl alcohol
PMA	Poly(methylmethacrylate)
PPy	Polypyrrole
PSS	Poly(styrene-4-sulfonate)
PTh	Polythiophene
R_{ct}	Charge transfer resistance
RuO_2	Ruthenium oxide
$RuO_x{\cdot}nH_2O$	Hydrous ruthenium oxide
rGO	Reduced graphene oxide
SWCNT	Single-walled carbon nanotubes
TM	Thermal management
XRD	X-ray diffraction
QGN	Quasi-graphene
VACNT	Vertically aligned carbon nanotubes

Introduction

Supercapacitors can be divided into two sections: pseudocapacitors and electrochemical double-layer capacitors (EDLC) by means of their energy storage mechanisms [1, 2]. Metal oxides are used to prepare electroactive materials for supercapacitors due to enhancing of their higher energy and power density capabilities [3, 4]. These materials have both deposit energy and supply Faradaic reactions [5]. We mostly reviewed ruthenium oxide (RuO_2), which were used in many studies due to its high capacitance, large voltage range, reversibility, good conductivity, and high charge/discharge capability [6, 7]. RuO_2 and its composites have Faradaic redox reactions via cyclic voltammetry (CV) method, which is a broad quasi-reversible rectangular box shape [8]. The specific capacitance (C_{sp}) of RuO_2 was obtained as $C_{sp}=700$ F/g in the literature [9–11]. The nanocomposites of metal oxides such as RuO_2, Co_3O_4, V_2O_5, and NiO and carbon-based materials were given as electrode materials for supercapacitors [12–14]. The inner d orbitals are responsible for the metallic conduction between ruthenium and oxygen elements [15].

Nanocomposites with RuO_2

Nanofillers and nanographene platelets have important effect to stabilize the nanocomposites [16]. In the literature, we have found that the addition of IrO_2 to RuO_2 improved the capacitive performance and cycle life of the thermally prepared Ir-Ru oxide coatings [17]. RuO_2 has been mostly employed in supercapacitor applications due to its high conductivity and reversibility processes [18–21]. However, there are some drawbacks associated with RuO_2 such as oxide delamination which are attributed to the breaking of the surface in acidic media [22–25]. Therefore, new composite materials were synthesized to develop the electrochemical performance and stability of RuO_2. Active carbon [26], carbon aerogel [27], carbon black [28], carbon nanotubes (CNTs) [29], graphene [30], conducting polymers [31], and metal oxides [32] have been extensively studied as supercapacitors in the literature [33, 34]. RuO_2 is used as a pseudocapacitor in supercapacitor [35, 36]. There is an important strategy to obtain higher capacitance by using a large surface area of materials [37]. rGO/RuO_2 nanocomposites has a capacitance value of $C_{sp}=879.1$ F/g at 0.5 A/g. Moreover, the specific capacitance was maintained over 98% for carbon nanotubes or reduced graphene oxide at 1 A/g. Shu et al. [38] indicated that MoN and Mo_2N showed capacitive behavior very similar to RuO_2. IrO_2 has also similar capacitance value compared to RuO_2 [39].

Zhang et al. [40, 41] reported composite structures containing RuO_2 and carbon materials, which are used as next-generation supercapacitor. Ambare et al. [42] stated metal oxides of Co_3O_4 and RuO_2. Results show that the highest C_{sp} was obtained as 628.33 F/g at 1 mV/s in 1 M KOH. Both materials Co_3O_4 [43] and RuO_2 [44, 45] show p-type semiconducting nature. Lee et al. [46] showed RuOx/polypyrrole nanocomposite which had C_{sp} values to be $C_{sp}=681$ F/g at 10 mV/s in 0.1 M H_2SO_4. The Ru% incorporation into the composite material affects the voltage range [47]. In the literature, the percent amount of RuO_2 in the total weight percent, C_{sp} was found to be 633 F/g for RuO_2/ordered mesoporous carbon structure [48].

Terasawa et al. [49] presented the incorporation of metal oxide particles such as RuO_2, NiO_2, MnO_2, or IrO_2 [50] with carbon materials. 1 wt% of RuO_2 into multi-walled carbon nanotubes (MWCNTs) electrode can increase the C_{sp} from 30 to 80 F/g. In addition, the relationship between charge/discharge ratio performance is higher than polymer/CNT composites [51]. Wang et al. [52] fabricated a supercapacitor device by plasma etching method. The results showed that a specific capacitance was found to be $C_{sp} = 272$ mF/cm^2 at 5 mV/s in neutral Na_2SO_4 solution. Figure 1 presents the CV of all electrocoated samples including modified electrodes given at 20 mV/s [53].

Commercial value of RuO_2

Thermal management (TM) has an important effect on electronic devices due to its performance and reliability of the devices [54]. The main aim is to obtain photoelectrochemical devices which have an efficiency of 8.5% [55]. Vita et al. [56] reported the activity of Pt/CeO_2 as a catalysts, which were studied toward the stream reforming (SR) of n-dodecane, used as surrogate fuel for marine diesel.

Transition metal oxides are important candidates for pseudocapacitance; however, RuO_2 and its composites are very expensive [57]. To circumvent this problem, more economic materials have been employed such as MnO_2 [58]. Xiong et al. [59] developed ternary cobalt ferrite/graphene/polyaniline composite for energy storage applications in industry. Aqueous electrolytes have some disadvantageous such as small voltage range (~ 1 V) [60]. This problem may be solved via using metal oxides such as RuO_2 [61].

RuO_2 is the most widely used metal oxide due to its high conductivity, capacitance, and chemical stability [62]. RuO_2 has been widely studied as an electrode material for electrochemical capacitance applications [63]. However, there are major limitations to its commercial applications due to its elevated cost [64]. Therefore, the commercialization is not promising due to its high cost as well as toxic effects [65–67].

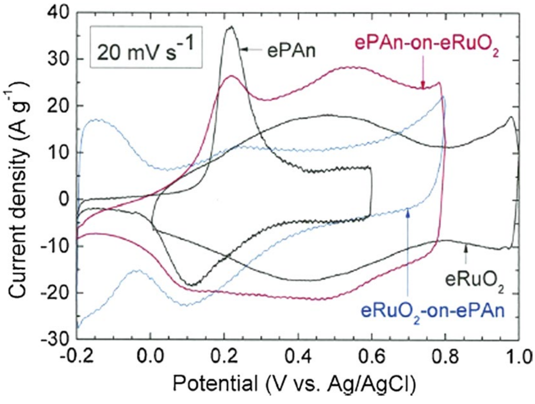

Fig. 1 CV of the electrocoated electrodes at 20 mV/s in 1.0 M H_2SO_4 electrolyte. Reprinted with permission from Ref. [53]. Copyright@Elsevier

RuO_2 and carbon fibers

The composites including micro-sized continuous fibers together with nano-sized fillers such as carbon nanotubes have limited studies which include these materials effects in the prediction of fracture energy [68]. Carbon fibers (CFs) have been employed for biosensor applications such as synthesis of poly(epsilon-caprolactone) (PCL)-based nanocomposite films [69]. Graphene fibers have been used for coating in textile industry for supercapacitor applications [70]. The hybrid fiber with a polyvinyl alcohol (PVA)/graphene oxide (GO) composites in the weight ratio of 10/90 has a capacitance of $C_{sp} = 241$ F/cm^3 in 1 M H_2SO_4.

Yang et al. [71] have prepared RuO_2/AC nanofibers by electrospinning method and thermal process. It shows good morphology and high C_{sp} value as 180 F/g. In addition, high energy density between $E = 14$ Wh/kg and $E = 20$ Wh/kg and high power density range were obtained as $P = 400$–10,000 W/kg in aqueous KOH electrolyte. A number of RuO_2 nanocomposites have been reported in the literature [72–74]. Chervin et al. [75] synthesized a self-limiting conformal RuO_2 film that coated around the nanofibers via silica paper in aqueous electrolyte [76]. RuO_2-containing mesoporous active carbon nanofiber (ACNF) composites were obtained by electrospinning, and then it was used as a supercapacitor application [77].

Fam et al. [78] stated a single-walled carbon nanotube (SWCNT)/RuO_2 or MnO_2 composites on glass fiber for supercapacitor. The specific capacitances were obtained as $C_{sp} = 72$ F/g for the SWCNT/MnO_2 and $C_{sp} = 98$ F/g for SWCNT/RuO_2. Liu et al. [79] identified that RuO_2 and MnO_2 had high capacities of $C_{sp} = 824$ F/g in 1 M H_2SO_4 and 1080 F/g in 2 M LiOH. Kim et al. [80] synthesized active carbon nanofiber with RuO_2 by electrospinning via poly(methyl methacrylate) (PMMA) for supercapacitors. The TEM images showed hollow spheres which were made up of carbon fiber (Fig. 2a). The EDS spectra are shown in Fig. 2b, where carbon, oxygen, and ruthenium elements exist in the polymer matrix. Only carbon and oxygen elements were observed in blue line of Fig. 2c. However, ruthenium element was not observed in amorphous phase of RuO_2 [81] (Fig. 2d). Moreover, two composite materials were shown in a broad and clear peak between 20° and 30° in X-ray diffraction (XRD) spectroscopy (Fig. 2e).

RuO_2 and carbon nanotubes

Nowdays, the interest of the carbon nanotube usage increased to aerospace technology [82]. Therefore, new substances were obtained in the form of film formation with nanomaterials inside the composite matrices [83]. CNTs are used toward the solubilization of chemical and physical modifications [84] and synthesis of materials [85]. CNTs have a unique chemical structure, which have high electrical and thermal conductivity, high chemical stability, and a high surface-to-volume ratio [86, 87]. CNTs have good mechanical properties, such as a high

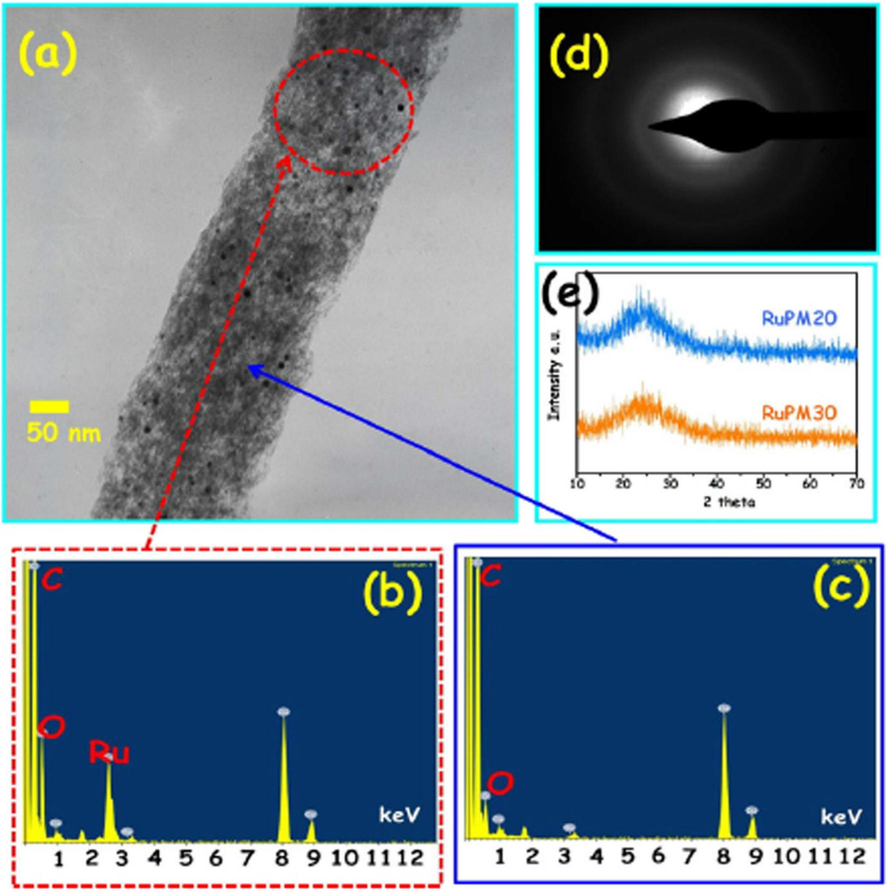

Fig. 2 TEM images **b**, **c** EDX data, **d** SEAD pattern of RuPM30, and **e** XRD peaks of RuPM30 and RuPM20. Reprinted with permission from Ref. [80]. Copyright@Elsevier

Young's modulus, high tensile strength, and high elongation at break [88]. The combination of RuO_2 and CNT mesoporous carbon provides an enhancement of the $C_{sp} = 1102$ F/g, $E = 0.15$ Wh/kg and $P = 0.237$ W/g values. These values are greater than mesoporous carbon. Lo et al. [89] studied the particle size of RuO_2 (10 wt%) to be ~2–5 nm which affects the increase of capacitance from 281 to 890 F/g at 2 mV/s. The carbon-based nanocomposites also support the capacitance results [90, 91]. Wu et al. [92] investigated three-dimensional hydrous RuO_2 nanotubes on Ti electrode at 90 °C [93]. Moreover, there is any binder usage in this study. The specific capacitance of RuO_2 nanotubes had a value of 745 F/g at 32 A/g. The electrode's retention was obtained to be 88.7% compared to the value of 840 F/g at 2 A/g. Chaitra et al. [94] synthesized RuO_2 and RuO_2/MWCNT nanocomposites by a simple hydrothermal method. The C_{sp} values of RuO_2 and RuO_2/MWCNT were presented to be 604 and 1585 F/g, respectively, at

2 mV/s in the voltage range from 0 to 1.2 V. Liu et al. [95] reported the functionalization of MWCNTs using 1-4-diaminoanthraquinone (DAAQ) and the synthesis of Pt-RuO_2 nanoparticles with different morphologies on DAAQ-MWCNTs by a microwave-assisted polyol method. Jung et al. [96] presented a vertically aligned carbon nanotubes (VACNT)/RuO_2 core–shell cathode for non-aqueous Li-O_2 batteries (Fig. 3). The VACNT is synthesized via chemical vapor deposition (CVD) method and used as the core material to obtain a binder-free and hierarchical porous structure.

RuO_2 and graphene nanosheets

Graphene (GN) has a carbon-based material which constitutes of a few layers of graphite nanocrystals. It supplies a synergetic effect in composite materials to enhance mechanical and capacitive properties [97]. Hu et al. synthesized rGO/RuO_2 hydrogel nanocomposites by hydrothermal technique in which RuO_2 had a particle size of 2–3 nm [98]. Hwang et al. [99] reported a simple laser-scribed rGO/RuO_2 nanocomposites for supercapacitors. Its C_{sp} and E values were

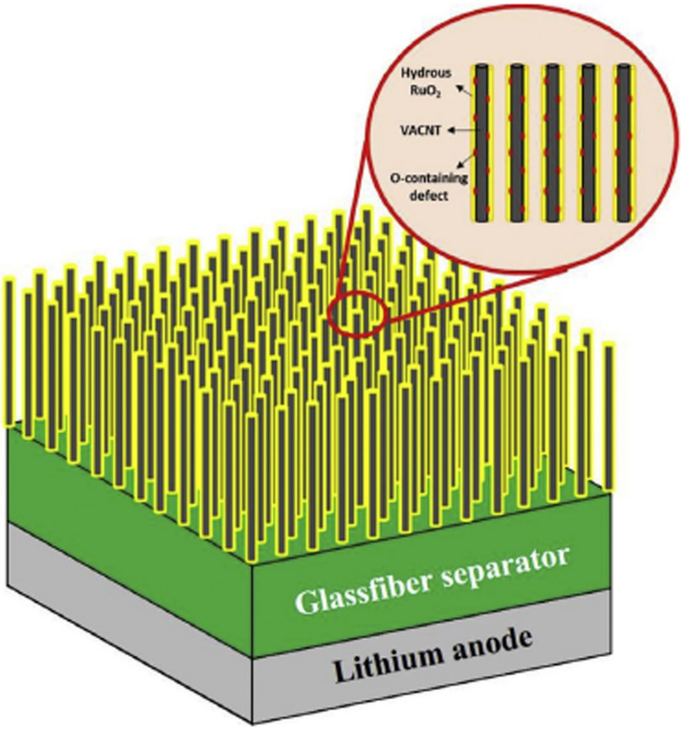

Fig. 3 Schematic illustration of the VACNT and RuO_2 cathode employed in a non-aqueous Li-O_2 battery. Reprinted with permission from Ref. [96]. Copyright@Elsevier

obtained to be $C_{sp} = 1139$ F/g and $E = 55.3$ Wh/kg. Leng et al. [100] made a nanocomposite of rGO/RuO_2/TiO_2, which had a facile in situ co-assembly without any surfactants. Ensafi et al. [101] synthesized Ni–Al/layered double hydroxide on GO and RuO_2 coated on GO. The RuO_2/graphene nanocomposite showed a good C_{sp} as 528.5 F/g at 0.1 A/g with a minimum charge transfer resistance (R_{ct}) of 0.4 Ω, an excellent rate capability as well as cycling stability [102]. Amir et al. [103] reported the synthesis of RuO_2/rGO nanocomposites via sol–gel method, followed by the electrophoretic deposition (EPD) of the material into thin films. The SEM and TEM images of rGO/RuO_2 films are shown in Fig. 4. Each nanosheet was fully coated with ultra-small RuO_2 nanoparticles. Moreover, the mean size of RuO_2 nanoparticles was found to be between 1.0 and 2.0 nm, homogeneously coated on the rGO.

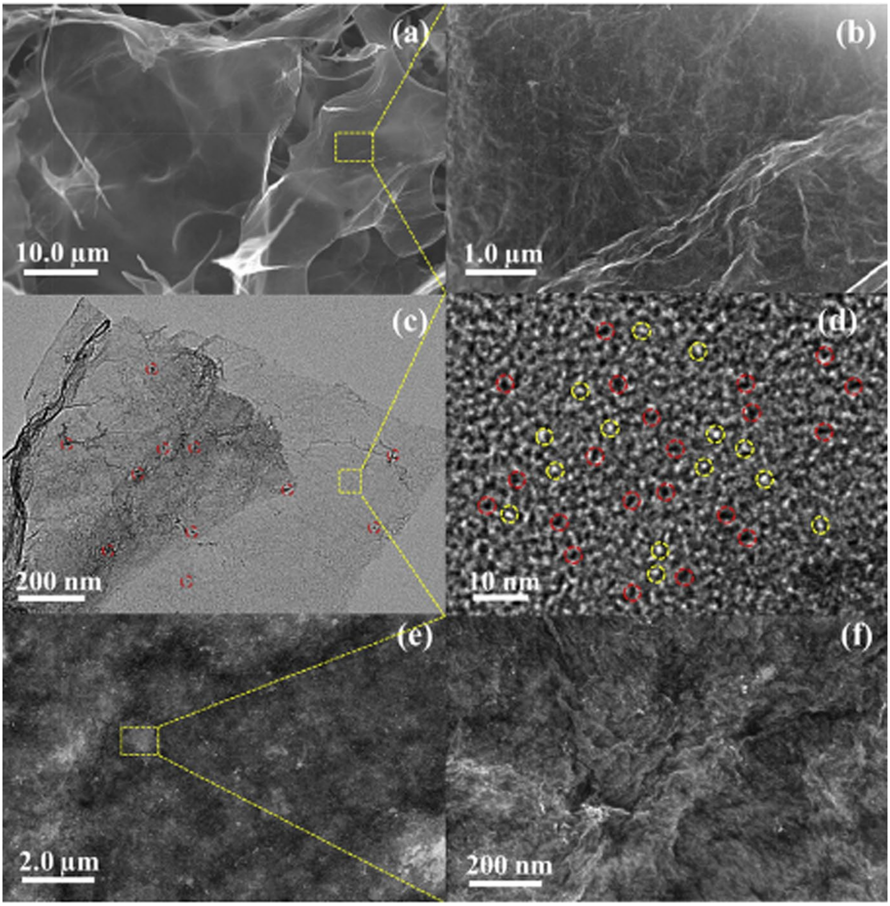

Fig. 4 **a**, **b** SEM images of freeze-dried HRGO-RuO_2, **c**, **d** TEM images of HRGO-RuO_2 (yellow and red circles were used to highlight the representative RuO_2 nanoparticles and the in-plane nanopores, respectively, and **e**, **f** SEM images of the surface of HRGO/RuO_2 film electrochemically deposited on gold coated PET (color figure online). Reprinted with permission from Ref. [103]. Copyright@Elsevier

RuO_2 and nanofiller-reinforced conducting polymers

The combination of nanofillers with polymer matrix showed the improvements of dielectric constant and lower loss tangent values [104]. Moreover, it supplies mechanical, dielectric, and thermal properties of polymer, which was followed by X-ray transmission electron microscopy for the morphology of nanofillers. In the literature, a nanocomposite of cerium oxide (CeO_2) dispersed in polyethylene oxide (PEO) polyethylene glycol (PEG) polymer electrolyte was prepared by standard solution casting method [105]. Graphite nanofibers [106], carbon nanotubes [107], carbon nanofibers [108], and graphene nanoplatelets [109] were used as nanofillers for preparing high-conductivity composite phase-change materials (PCM).

Conducting polymers already has been used as an active electrode material in supercapacitors [110]. However, there are some disadvantageous associated to it, such as low stability and limited capacitance, causing limited commercial applications. To solve these problems, conducting nanofillers were added to nanocomposite materials so that the conductivity and capacitance of the active electrode material would be increased. Lean et al. [111] studied the energy storage systems of nanofillers. In the literature, a mesoporous silica MCM-48 was added to poly(methyl acylate) (PMA) to improve mechanical and thermophysical properties [112]. This material in polymer shows a good dielectric constant and lower loss tangent values [113]. In general, nanofiller materials enhance the performance of nanocomposites in various applications [114]. Ann et al. [115] reported PPy hollow nanoparticles as the specific capacitance of $C_{sp} = 326\ Fg^{-1}$, which had two times higher than PPy. Its charge/discharge capacitance retention was obtained to be 86% even following 10.000 cycles.

Pseudocapacitors based on RuO_2

Pseudocapacitors based on Faradaic redox reactions have been reviewed in the literature [116, 117]. These redox reactions occur such as polyaniline, polypyrrole, MnO_2, and RuO_2 [118–120]. Anodic pseudocapacitors have been developed for many types of metal oxides [121]. The C_{sp} values show up to 700 F/g [122, 123]. RuO_2 is one of the most used metal oxides due to easy synthesis, high theoretical capacitance ($C_{sp} = 1358$ F/g) [124], rapid charge/discharge processes, long life cycle [125, 126], and high gravimetric capacity [127]. $RuO_2 \cdot xH_2O$ has been synthesized by vapor-phase deposition from RuO_4 [128–130].

RuO_2 has high C_{sp} values from 1300 to 2200 F/g for pseudocapacitor applications, [131, 132] and high electrical conductivity (10^5 S/cm) [133–135]. As it is an expensive metal oxide the more economic metal oxides such as MnO_2, NiO, and Co_3O_4 have been used with C_{sp} values of 698 F/g [136–140]. Arnold et al. [141] presented a laser scribing to obtain hydrous ruthenium oxide for supercapacitors. Sopcic et al. [142] studied the capacitance performance of RuO_2 which was measured by CV and electrochemical quartz crystal nanobalance (EQCN) in H_2SO_4, Na_2SO_4 and K_2SO_4 solution. Nguyen et al. [143] investigated RuO_2 electrodes by CV method and investigation of protic ionic liquids in supercapacitor device (Fig. 5).

RuO_2-based symmetric and asymmetric supercapacitors

Supercapacitors have higher capacitance, energy, and power densities than batteries [144, 145]. There are some advantages for using hydrous ruthenium oxide ($RuO_x \cdot nH_2O$) such as ultra-high pseudocapacitance [146], wide potential range of stability, charge/discharge performance, and good cycle life [147]. Crystalline RuO_2 has poor capacitance despite of d-band metallic conductor [148]. However, amorphous RuO_2 has high capacitance as $C_{sp} = 720$ F/g.

Nanostructured RuO_2 materials have been synthesized using a great variety of methods, such as chemical precipitation, potentiostatic, potentiodynamic coating, hydrothermal and chemical vapor deposition, electrolytic methods and electrostatic spray deposition [149, 150]. These materials are used in a symmetric/asymmetric supercapacitor device fabrication. For instance, carbon fiber (CF) modified with anthraquinone (AQ)/RuO_2 nanocomposite was obtained as $E = 12.7$ Wh/kg [151]. RuO_2 and Co_3O_4 metal oxides on CF showed good electrochemical performance with $E = 1.44$ Wh/cm^3 and $P = 0.89$ W/cm^3.

The reversible reaction shown during charge/discharge process is presented below:

$$MN + 3Li^+ + 3e^- \leftrightarrow M + Li_3N$$

Such phase transformation in case of metal nitrides MN (M = Cr, Co) are not observed when cycled against carbon electrode materials, like RuO_2 [152], which is used as electrode materials for supercapacitors [153]. Zhang et al. [154] studied transparent, electroactive materials with RuO_2/PEDOT:PSS (Fig. 6).

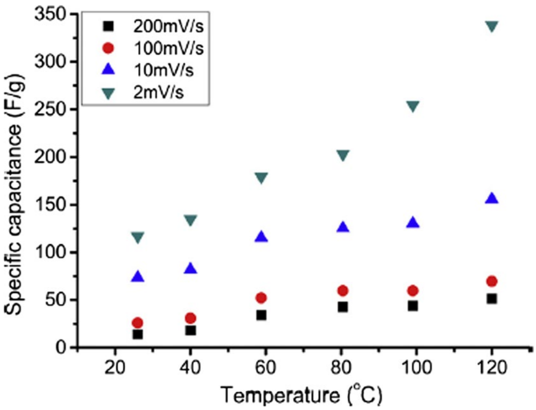

Fig. 5 Specific capacitance is increased by increasing the temperature. The values were calculated using the anodic current from the cyclic voltammograms. Reprinted with permission from Ref. [143]. Copyright@Elsevier

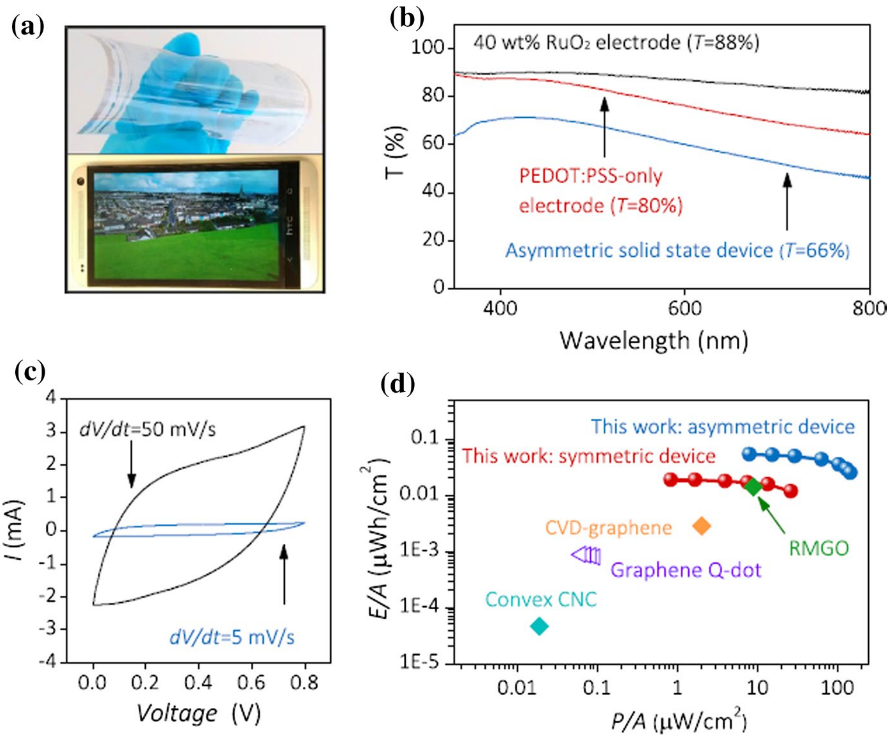

Fig. 6 **a** Photograph of flexible asymmetric solid-state supercapacitor and the same device overlaid on a mobile phone display. **b** Transmittance spectra of the constituent electrodes and the complete device (with the same solid electrolyte). **c** CVs of the device at 5 mV/s. **d** Ragone plot for the 40 wt% RuO_2-based solid-state symmetric and asymmetric devices featured in this work, along with values for other devices described in the literature. Reprinted with permission from Ref. [154]. Copyright@Elsevier

A table was obtained from the literature reports of this review article reports on RuO_2-carbon-based conducting polymer nanocomposites for supercapacitors during the years 2000–2017 as shown in Table 1.

Concluding remarks

This review article summarizes the nanocomposites with RuO_2 such as carbon fibers, carbon nanotubes, and graphene nanosheets. Economical value of RuO_2 was presented in this study. Moreover, pseudocapacitance behaviors of RuO_2-based symmetric and asymmetric supercapacitors were given in this study. As a result, RuO_2 is an expensive metal oxide but has higher capacitive behaviors in various nanomaterials compared to other metal oxides, such as NiO_2, TiO_2.

Table 1 Literature reports on ruthenium oxide–carbon-based conducting polymer nanocomposites for supercapacitors during the years 2000–2017

System	Electrolyte	Capacitance/(F/g)	References
$RuCo_2O_4$	KOH	1469 F/g at 6 A/g	[9]
Hydrous RuO_2	1 M H_2SO_4	977 F/g at 1 mA	[20]
Ru/carboxylated graphene	0.5 M H_2SO_4	756 F/g by CV	[34]
$RuO_2 \times H_2O$/CF	2 M H_2SO_4	440 F/g at 23 mA/cm^2	[36]
RuO_2/Co_3O_4	1 M KOH	628.33 F/g at 1 mV/s	[42]
RuO_2 in amorphous phase	0.5 M H_2SO_4	551 F/g at 5 mV/s	[44]
RuO_x/PPy	0.1 M H_2SO_4	478 F/g at 10 mV/s	[46]
RuO_2/Fe_2O_3	1 M H_2SO_4	1668 F/g	[48]
RuO_2/ACNFs	1 M KOH	180 F/g	[71]
RuO_2/graphene	1 M H_2SO_4	528.5 F/g at 0.1 A/g	[102]
HRGO/RuO_2	PVA-H_2SO_4	418 F/g at 1 A/g	[103]
QGN/RuO_2	1 M KOH	453.7 F/g	[116]
RuO_2/AC 20 wt% RuO_2	1 M H_2SO_4	260 F/g	[137]

Compliance with ethical standards

Conflict of interest There is no conflict of interest in this review article.

References

1. Guo XL, Kuang M, Li F, Liu XY, Zhang YX, Dong F, Losic D (2016) Engineering of three-dimensional (3-D) diatom@TiO_2@MnO_2 composites with enhanced supercapacitor performance. Electrochim Acta 190:159–167
2. Guo XL, Li G, Kuang M, Yu L, Zhang YX (2015) Tailoring Kirkendall effect of the KCu_7S_4 microwires towards CuO@MnO_2 core-shell nanostructures for supercapacitors. Electrochim Acta 174:87–92
3. Patake VD, Lokhande CD, Joo OS (2009) Electrodeposited ruthenium oxide thin films for supercapacitors: effects of surface treatments. Appl Surf Sci 255:4192–4196
4. Brezesinski T, Wang J, Tolbert SH, Dunn B (2010) Ordered mesoporous alpha-MoO_3 with iso-oriented nanocrystalline walls for thin pseudocapacitors. Nat Mater 9:146–151
5. Zhao DD, Bao SJ, Zhou WH, Li HL (2007) Preparation of hexagonal nanoporous nickel hydroxide film and its application for electrochemical capacitor. Electrochem Commun 9:869–874
6. Kim IH, Kim KB (2006) Electrochemical characterization of hydrous ruthenium oxide thin-film electrodes for electrochemical capacitor applications. J Electrochem Soc 153:A383–A389
7. Sugimoto W, Yokoshima K, Murakami Y, Takasu Y (2006) Charge storage mechanism of nanostructured anhydrous and hydrous ruthenium-based oxides. Electrochim Acta 52:1742–1748
8. Augustyn V, Simon P, Dunn B (2014) Pseudocapacitive oxide materials for high-rate electrochemical energy storage. Energy Environ Sci 7:1597–1614
9. Dubal DP, Chodankar NR, Holze R, Kim DH, Gomez-Romero P (2017) Ultrathin mesoporous $RuCo_2O_4$ nanoflakes: an advanced electrode for high-performance symmetric supercapacitors. Chemsuschem 10:1771–1782
10. Bi RB, Wu XL, Cao FF, Jiang LY, Guo YG, Wan LJ (2010) Highly dispersed RuO_2 nanoparticles on carbon nanotubes: facile synthesis and enhanced supercapacitance performance. J Phys Chem C 114:2448–2451

11. Rakhi RB, Chen W, Hedhili MN, Cha D (2014) Enhanced rate performance of mesoporous Co_3O_4 nanosheet supercapacitor electrodes by hydrous RuO_2 nanoparticles decoration. ACS Appl Mater Interfaces 6:4196–4206
12. Liang J, Tan H, Xiao C, Zhou G, Guo S, Ding S (2015) Hydroxyl-riched halloysite clay nanotubes serving as substrate of NiO nanosheets for high-performance supercapacitor. J Power Sources 285:210–216
13. Nair DP, Sakthivel T, Nivea R, Eshow JS, Gunasekaran V (2015) Effect of surfactants on electrochemical properties of vanadium pentaoxide nanoparticles synthesized via hydrothermal method. J Nanosci Nanotechnol 15:4392–4397
14. Hu Z, Zu L, Jiang Y, Lian H, Liu Y, Li Z, Chen F, Wang X, Cui X (2015) High specific capacitance of polyaniline/mesoporous manganese dioxide composite using KI-H_2SO_4 electrolyte. Polymers 7:1939–1953
15. Lei BH, Kong QR, Yang ZH, Yang Y, Wang Y, Pan SL (2016) Hierarchized band gap and enhanced optical responses of trivalent rare-earth metal nitrates due to (d–p) pi conjugation interactions. J Mater Chem C 4:6295–6301
16. Borjanovic V, Bistricic L, Pucic I, Mikac L, Slunjski R, Jaksic M, McGuine G, Stankovic AT, Shenderova O (2016) Proton-radiation resistance of poly(ethylene terephthalate)-nanodiamond-graphene nanoplatelet nanocomposites. J Mater Sci 51:1000–1016
17. Ullah N, McArlhur MA, Omanovic S (2015) Iridium-ruthenium oxide coatings for supercapacitors. Can J Chem Eng 93:1941–1948
18. Hu CC, Chang KH (2000) Cyclic voltammetric deposition of hydrous ruthenium oxide for electrochemical capacitors: effects of codepositing iridium oxide. Electrochim Acta 45:2685–2696
19. Fisher RA, Watt MR, Jud Ready W (2013) Functionalized carbon nanotubes supercapacitor electrode: a review on pseudocapacitive materials. ECS J Solid State Sci Technol 2:M3170–M3177
20. Liu X, Pickup PG (2008) Ru oxide supercapacitors with high loadings and high power and energy densities. J Power Sources 176:410–416
21. Panic VV, Dekanski AB, Nikolic BZ (2013) Tailoring the supercapacitive performances of noble metal oxides, porous carbons and their composites. J Serb Chem Soc 78:2141–2164
22. Lokhande CD, Dubal DP, Joe OS (2011) Metal oxide thin film based supercapacitors. Curr Appl Phys 11:255–270
23. Liu CC, Tsai DS, Susanti D, Yeh WC, Huang YS, Liu FJ (2010) Planar ultracapacitors of miniature interdigital electrode loaded with hydrous RuO_2 and RuO_2 nanorods. Electrochim Acta 55:5768–5774
24. Yang XF, Wang GC, Wang RY, Li XW (2010) A novel layered manganese oxide/poly(aniline-co-o-anisidine) nanocomposite and its application for electrochemical supercapacitor. Electrochim Acta 55:5414–5419
25. Nikolic BZ, Panic VV, Dekanski AB (2012) Intrinsic potential dependent performances of a sol–gel prepared electrocatalytic IrO_2–TiO_2 coating of dimensionally stable anodes. Electrocatalysis 3:360–368
26. Ni Y, Xu J, Liang Q, Shao SJ (2017) Enzyme-free glucose sensor based on heteroatom-enriched activated carbon (HAC) decorated with hedgehog-like NiO nanostructures. Sens Actuators B Chem 250:491–498
27. Yu M, Han Y, Li J, Wang L (2017) One-step synthesis of sodium carboxymethyl cellulose-derived carbon aerogel/nickel composites for energy storage. Chem Eng J 324:287–295
28. Yang CC, Tsai MH, Huang CW, Yen PJ, Pan CC, Wu WW, Wei KH, Dung LR, Tseng TY (2017) Carbon nanotube/nitrogen-doped reduced graphene oxide nanocomposites and their application in supercapacitors. J Nanosci Nanotechnol 17:5366–5373
29. Yao Z, Meng Y, Xia Q, Li D, Zhao Y, Li C, Jiang Z (2017) Synthesis of carbon modified TiO_2 nanotubes composite films by gas thermal penetration as symmetrical and binder-free electrochemical supercapacitor. J. Alloys Compd 721:795–802
30. Wei YX, Ding RM, Zhang CH, Lv BL, Wang Y, Chen CM, Wang XP, Xu J, Yang Y, Li YW (2017) Facile synthesis of self-assembled ultrathin alpha-FeOOH nanorod/graphene oxide composites for supercapacitors. J Colloid Interface Sci 504:593–602
31. Bae J, Park JY, Kwan OS, Lee CS (2017) Energy efficient capacitors based on graphene/conducting polymer hybrids. J Ind Eng Chem 51:1–11
32. Khandare L, Terdale S (2017) Gold nanoparticles decorated MnO_2 nanowires for high performance supercapacitor. Appl Surf Sci 418:22–29

33. Wang X, Liu P (2014) Improving the electrochemical performance of polyaniline electrode for supercapacitor by chemical oxidative copolymerization with p-phenylene daimine. J Ind Eng Chem 20:1324–1331
34. Meng Y, Wang L, Xiao H, Ma Y, Chao L, Xie Q (2016) Facile electrochemical preparation of composite film of ruthenium dioxide and carboxylated graphene for a high performance supercapacitors. RSC Adv 6:33666–33675
35. Vellacheri R, Pillai VK, Kurungot S (2012) Hydrous RuO_2-carbon nanofiber electrodes with high mass and electrode specific capacitance for efficient energy storage. Nanoscale 4:890–896
36. Pico F, Ibanez J, Lillo-Rodenas MA, Linares-Solano A, Rojas RM, Amarilla JM, Rojo JM (2008) Understanding RuO_2 center dot xH(2)O/carbon nanofiber composites as supercapacitor electrodes. J Power Sources 176:417–425
37. Wang P, Liu H, Xu Y, Chen Y, Yang J, Tan Q (2016) Supported ultrafine ruthenium oxides with specific capacitance up to 1099 F g^{-1} for a supercapacitor. Electrochim Acta 194:211–218
38. Shu Y, Xu J, Chen JY, Xu Q, Xiao X, Jin DQ, Pang H, Hu XY (2017) Ultrasensitive electrochemical detection of H_2O_2 in living cell based on ultrathin MnO_2 nanosheets. Sens Actuators B Chem 252:72–78
39. Shao YQ, Chen ZJ, Zhu JQ, Zhang S, Lin DY, Yi ZY, Tang D (2016) Relationship between electronic structures and capacitive performance of the electrode material. J Am Ceram Soc 99:2504–2511
40. Zhang Y, Park SJ (2017) Incorporation of RuO_2 into charcoal-derived carbon with controllable microporosity by CO_2 activation for high-performance supercapacitor. Carbon 122:287–297
41. Ma HY, Kong DB, Xu Y, Xie XY, Tao Y, Xiao ZC, Lv W, Jang HD, Huang JX, Yang QH (2017) Disassembly–reassembly approach to RuO_2/graphene composites for ultrahigh volumetric capacitance supercapacitor. Small 13, Article number: UNSP1701026
42. Ambare RC, Bharadwaj SR, Lokhande BJ (2015) Non-aqueous route spray pyrolyzed Ru:Co_3O_4 thin electrodes for supercapacitor application. Appl Surf Sci 349:887–896
43. Shinde VR, Mahadik SB, Gujar TP, Lokhande CD (2006) Supercapacitive cobalt oxide (Co_3O_4) thin films by spray pyrolysis. Appl Surf Sci 252:7487–7492
44. Gujar TP, Shinde VR, Lokhande CD, Kim WY, Jung KD, Joo OS (2007) Spray deposited amorphous RuO_2 for an effective use in electrochemical supercapacitor. Electrochem Commun 9:504–510
45. Wang P, Liu H, Tan Q, Yang J (2014) Ruthenium oxide-based nanocomposites with high specific surface area and improved capacitance as a supercapacitor. RSC Adv 4:42839–42845
46. Lee H, Cho MS, Nam ID, Lee Y (2010) RuOx/polypyrrole nanocomposite electrode for electrochemical capacitors. Synth Met 160:1055–1059
47. Hu CC, Chang KH, Lin MC, Wu YT (2006) Design and tailoring of the nanotubular arrayed architecture of hydrous RuO_2 for next generation supercapacitors. Nano Lett 6:2690–2695
48. Xiang D, Yin L, Wang C, Zhang L (2016) High electrochemical performance of RuO_2–Fe_2O_3 nanoparticles embedded ordered mesoporous carbon as a supercapacitor electrode material. Energy 106:103–111
49. Terasawa N, Mukai K, Yamato K, Asaka K (2012) Superior performance of non-activated multi-walled carbon nanotube polymer actuator containing ruthenium oxide over a single-walled carbon nanotubes. Carbon 50:1888–1896
50. Terasawa N, Asaka K (2014) High-performance hybrid (electrostatic double-layer and faradaic capacitor based) polymer actuators incorporating nickel oxide and vapor-grown carbon nanofibers. Langmuir 30:14343–14351
51. Arabale G, Wagh D, Kulkarni M, Mulla I, Vernekar S, Vijayamoharan K, Rao AM (2003) Enhanced supercapacitance of multiwalled carbon nanotubes functionalized with ruthenium oxide. Chem Phys Lett 376:207–213
52. Wang X, Yin Y, Hao C, You Z (2015) A high-performance three-dimensional microsupercapacitor based on ripple-like ruthenium oxide-carbon nanotube composite films. Carbon 82:436–445
53. Kim KM, Lee YG, Shin DO, Ko JM (2016) Supercapacitive properties of layered electrodes composed of electrodeposited RuO_2 and polyaniline. Electrochim Acta 196:309–315
54. Mortazavi B, Yang HL, Mohebbi F, Cuniberti G, Rabczuk T (2017) Graphene or h-BN paraffin composite structures for the thermal management of Li-ion batteries: a multiscale investigation. Appl Energy 202:323–334
55. Guldi DM, Rahman GMA, Zerbetto F, Prato M (2005) Carbon nanotubes in electron donor–acceptor nanocomposites. Acc Chem Res 38:871–878

56. Vita A, Italiano C, Fabiano C, Pino L, Lagana M, Recupero V (2016) Hydrogen-rich gas production by steam reforming of *n*-dodecane part I: catalytic activity of Pt/CeO_2 catalysts in optimized bed configuration. Appl Catal B Environ 199:350–360
57. Achilleos DS, Hatton TA (2015) Surface design and engineering of hierarchical hybrid nanostructures for asymmetric supercapacitors with improved electrochemical performance. J Colloid Interface Sci 447:282–301
58. Luo X, Yang JY, Yan D, Wang W, Wu X, Zhu ZH (2017) MnO_2-decorated 3D porous carbon skeleton devived from mollusc shell for high-performance supercapacitor. J Alloys Compd 723:505–511
59. Xiong P, Huang H, Wang X (2014) Design and synthesis of ternary cobalt ferrite/graphene/polyaniline hierarchical nanocomposites for high performance supercapacitors. J Power Sources 245:937–946
60. Naoi K, Ishimote S, Miyamoto J, Naoi W (2012) Second generation nanohybrid supercapacitor: evolution of capacitive energy storage devices. Energy Environ Sci 5:9363–9373
61. Naoi K, Simon P (2008) New materials and new configurations for advanced electrochemical capacitors. Electrochem Soc Interface 17:34–37
62. Xia H, Meng YS, Yuan G, Cui C, Lu L (2012) A symmetric RuO_2/RuO_2 supercapacitor operating at 1.6 V by using a neutral aqueous electrolyte. Electrochem Solid State Lett 15:A60–A63
63. Wu Z, Wang D, Ren W, Zhao J, Zhou G, Li F, Cheng H (2010) Anchoring hydrous RuO_2 on graphene sheets for high-performance electrochemical capacitors. Adv Funct Mater 20:3595–3602
64. Yousefi T, Golikand AN, Mashhadizadeh MH, Aghazadeh M (2012) Template-free synthesis of MnO_2 nanowires with secondary flower like structure: characterization and supercapacitor behavior studies. Curr Appl Phys 12:193–198
65. Zhao X, Sanchez BM, Dobson P, Grant P (2011) The role of nanomaterials in redox-based supercapacitors for next generation energy storage devices. Nanoscale 3:839–855
66. Rauda IE, Augustyn V, Dunn B, Tolbert SH (2013) Enhancing pseudocapacitive charge storage in polymer templated mesoporous materials. Acc Chem Res 46:1113–1124
67. Wu ZS, Wang DW, Ren W, Zhao J, Zhou G, Li F, Cheng HM (2010) Anchoring hydrous RuO_2 on graphene sheets for high-performance electrochemical capacitors. Adv Funct Mater 20:3595–3602
68. Menna C, Bakis CE, Prota A (2016) Effect of nanofiller length and orientation distributions on mode I fracture toughness of unidirectional fiber composites. J Compos Mater 50:1331–1352
69. Gopinathan J, Pillai MM, Elakkiya V, Selvakumar R, Bhattacharyya A (2016) Carbon nanofiller incorporated electrically conducting poly(elipson-caprolactone) nanocomposite films and their biocompatibility studies using MG-63 cell line. Polym Bull 73:1037–1053
70. Chen S, Ma W, Xiang H, Cheng Y, Yang S, Weng W, Zhu M (2016) Conductive, tough, hydrophilic poly(vinyl alcohol)/graphene hybrid fibers for wearable supercapacitors. J Power Sources 319:271–280
71. Yang KS, Kim CH, Kim BH (2015) Preparation and electrochemical properties of RuO_2-containing activated carbon nanofiber composites with hollow cores. Electrochim Acta 174:290–296
72. Sugimoto W, Kizaki T, Yokoshima K, Murakami Y, Takasu Y (2004) Evaluation of the pseudocapacitance in RuO_2 with RuO_2/GC thin film electrode. Electrochim Acta 49:313–320
73. Wang W, Guo S, Lee I, Ahmed K, Zhong J, Favors Z, Zaera F, Ozkan M, Ozkan CS (2014) Hydrous ruthenium oxide nanoparticles anchored to graphene and carbon nanotube hybrid foam for supercapacitors. Sci Rep 4, Article number: 4452
74. Ju YW, Choi GR, Jung HR, Kim C, Yang KS, Lee WJN (2007) A hydrous ruthenium oxide-carbon nanofibers composite electrodes prepared by electrospinning. J Electrochem Soc 154:A192–A197
75. Chervin CN, Lubers AM, Long JW, Rolison DR (2010) Effect of temperature and atmosphere on the conductivity and electrochemical capacitance of single-unit thick ruthenium dioxide. J Electroanal Chem 644:155–163
76. Ryan JV, Berry AD, Anderson ML, Long JW, Stroud RM, Cepak VM (2000) Electronic connection to the interior of a mesoporous insulator with nanowires of crystalline RuO_2. Nature 406:169–172
77. Kim BH, Kim CH, Lee DG (2016) Mesopore-enriched activated carbon nanofiber web containing RuO_2 as electrode material for high-performance supercapacitors. J Electroanal Chem 760:64–70
78. Fam DWH, Azoubel S, Liu L, Huang J, Mandler D, Magdassi S, Tok AIY (2015) Novel felt pseudocapacitor based on carbon nanotube/metal oxide. J Mater Sci 50:6578–6585
79. Liu X, Pickup PG (2011) Carbon fabric supported manganese and ruthenium oxide thin films for supercapacitors. J Electrochem Soc 158:A241–A249
80. Kim BH, Kim CH, Lee DG (2016) Mesopore-enriched activated carbon nanofiber web containing RuO_2 as electrode material for high-performance supercapacitors. J Electroanal Chem 760:64–70

81. Zhu Y, Ji X, Pan C, Sun Q, Song W, Fang L, Chen Q, Banks CE (2013) A carbon quantum dot decorated RuO_2 network:outstanding supercapacitors under ultrafast charge and discharge. Energy Environ Sci 6:3665–3675
82. Bouchard J, Cayla A, Odent S, Lutz V, Devaux E, Campagne C (2016) Processing and characterization of polyethersulfone wet-spun nanocomposite fibres containing mutiwalled carbon nanotubes. Synth Met 217:304–313
83. Bouchard J, Cayla A, Lutz V, Campagne C, Devaux E (2012) Electrical and mechanical properties of phenoxy/multiwalled carbon nanotubes multifilament yarn processed by melt spinning. Text Res J 82:2116–2125
84. Murakami H, Nakashima N (2006) Soluble carbon nanotubes and their applications. J Nanosci Nanotechnol 6:16–27
85. Nguyen DN, Yoon H (2016) Recent advances in nanostructured coonducting polymers: from synthesis to practical applications. Polymers 8, Article number: 118
86. Wei C, Srivastava D, Cho K (2002) Thermal expansion and diffusion coefficients of carbon nanotube-polymer composites. Nano Lett 3:647–650
87. Shin US, Knowles JC, Kim HW (2011) Positive charge doping on carbon nanotube walls and anion directed tunable dispersion of the derivatives. Bull Korean Chem Soc 32:1635–1639
88. Yoon IIK, Hwang JY, Jang WC, Kim HW, Shin US (2014) Natural bone-like biomimetic surface modification of titanium. Appl Surf Sci 301:401–409
89. Lo AY, Jheng Y, Huang TC, Tseng CM (2015) Study on RuO_2/CMK-3/CNTs composites for high power and high energy density supercapacitor. Appl Energy 153:15–21
90. Brown B, Cordova IA, Parker CB, Stone BR, Glass JT (2015) Optimization of active manganase oxide electrodeposits using graphenated carbon nanotube electrodes for supercapacitors. Chem Mater 27:2430–2438
91. Peng L, Peng X, Liu B, Wu C, Xie Y, Yu G (2013) Ultrathin two-dimensional MnO_2/graphene hybrid nanostructures for high performance, flexible planar supercapacitors. Nano Lett 13:2151–2157
92. Wu X, Xiong W, Chen Y, Lan D, Pu X, Zeng Y, Gao H, Chen J, Tong H, Zhu Z (2015) High-rate supercapacitor utilizing hydrous ruthenium dioxide nanotubes. J Power Sources 294:88–93
93. Li H, Wang R, Cao R (2008) Physical and electrochemical characterization of hydrous ruthenium oxide/ordered mesoporous carbon composites as supercaopacitor. Microporous Mesoporous Mater 111:32–38
94. Chaitra K, Sivaraman P, Vinny RT, Bhatta UM, Nagaraju N, Kathyayini N (2016) High energy density performance of hydrothermally produced hydrous ruthenium oxide/multiwalled carbon nanotubes composite: design of an asymmetric supercapacitor with excellent cycle life. J Energy Chem 25:627–635
95. Liu R, Luo Z, Wei Q, Zhou X (2016) Pt-RuO_2 nanoparticles supported on diaminoanthraquinone-functionalized carbon nanotubes as efficient catalysts for methanol oxidation. Mater Des 94:132–138
96. Jung CY, Zhao TS, Zeng L, Tan P (2016) Vertically aligned carbon nanotube-ruthenium dioxide core-shell cathode for non-aqueous lithium-oxygen batteries. J Power Sources 331:82–90
97. Hossain MK, Chowdhury NMR, Hosur M, Jeelani S, Bolden NW (2015) Enhanced properties of epoxy composite reinforced with amino-functionalized graphene nanoplateles. In: Proceedings of the ASME International Mechanical Engineering Congress and Exposition, 9, Article number: V009T12A072. Housten, TX, 13–19 Nov 2015
98. Yang Y, Liang Y, Zhang Y, Zhang Z, Li Z, Hu Z (2015) Three-dimensional graphene hydrogel supported ultrafine RuO_2 nanoparticles for supercapacitor electrodes. New J Chem 39:4035–4040
99. Hwang JY, El-Kady MF, Wang Y, Wang L, Shao Y, Marsh K, Ko JM, Kaner RB (2015) Direct preparation and processing of graphene/RuO_2 nanocomposite electrodes for high-performance capacitive energy storage. Nano Energy 18:57–70
100. Leng X, Liu R, Zou J, Xiong X, He H (2016) One-pot hydrothermal synthesis of graphene–RuO_2–TiO_2 nanocomposites. Mater Lett 166:175–178
101. Ensafi AA, Jafari-Asl M, Nabiyan A, Rezaei B (2016) Preparation of three-dimensional ruthenium oxide@graphene oxide based on etching of Ni–Al/layered double hydroxides: application for electrochemical hydrogen generation. J Electrochem Soc 163:H610–H617
102. Leng X, Zou J, Xiong X, He H (2015) Electrochemical capacitive behavior of RuO_2/graphene composites prepared under various precipitation conditions. J Alloys Compd 653:577–584

103. Amir FZ, Pham VH, Mullinax DW, Dickerson JH (2016) Enhanced performance of HRGO-RuO_2 solid state flexible supercapacitors fabricated by electrophoretic deposition. Carbon 107:338–343
104. Yaragalla S, Sindam B, Abraham J, Raju KCJ, Kalarikkal N, Thomas S (2015) Fabrication of graphite-graphene-ionic liquid modified carbon nanotubes filled natural rubber thin films for microwave and energy storage applications. J Polym Res 22, Article number: 137
105. Ali TM, Padmanathan N, Selladurai S (2015) Effect of nanofiller CeO_2 on structural, conductivity and dielectric behaviors of plasticized blend nanocomposite polymer electrolyte. Ionics 21:829–840
106. Sahan N, Fois M, Paksoy H (2015) Improving thermal conductivity phase change materials—a study of parafin nanomagnetite composites. Sol Energy Mater Sol Cells 137:61–67
107. Warzoha RJ, Fleischer AS (2015) Effect of carbon nanotube interfacial geometry on thermal transport in solid-liquid phase change materials. Appl Energy 154:271–276
108. Fan LW, Fang X, Wang X, Zeng Y, Xiao YQ, Yu ZT, Xu X, Hu YC, Cen KF (2013) Effects of various carbon nanofillers on the thermal conductivity and energy storage properties of parafin-based nanocomposite phase change materials. Appl Energy 110:163–172
109. Fan LW, Zhu ZQ, Zeng Y, Xiao YQ, Liu XL, Wu YY, Ding Q, Yu ZT, Cen KF (2015) Transient performance of a PCM-based heat sink with high aspect-ratio carbon nanofillers. Appl Therm Eng 75:532–540
110. Zhao ZH, Richardson GF, Meng QS, Zhu SM, Kuan HC, Ma J (2016) PEDOT-based composites as electrode materials for supercapacitors. Nanotechnology 27, Article number: 042001
111. Lean MH, Chu WPL (2016) Effective permittivity of nanocomposites from 3D charge transport simulations. J Appl Polym Sci 133, Article number: 43300
112. Perez LD, Giraldo LF, Brostow W, Lopez BL (2007) Poly(methyl acrylate) plus mesoporous silica nanohybrids: mechanical and thermophysical properties. E-Polymers, Article number: 029
113. Yaragalla S, Sindam B, Abraham J, Raju KCJ, Kalarikkal N, Thomas S (2015) Fabrication of graphite-graphene ionic liquid modified carbon nanotubes filled natural rubber thin films for microwave and energy storage applications. J Polym Res 22, Article number: 137
114. Nguyen DN, Yoon H (2016) Recent advances in nanostructured conducting polymers: from synthesis to practical applications. Polymers 8, Article number: 118
115. Ahn KJ, Lee Y, Choi H, Kim MS, Im K, Noh S, Yoon H (2015) Surfactant-templated synthesis of polypyrrole nanocages as redox mediators for efficient energy storage. Sci Rep 5, Article number: 14097
116. Zhang C, Zhou H, Yu X, Ye T, Huang Z, Kuang Y (2014) Synthesis of RuO_2 decorated quasi graphene nanosheets and their application in supercapacitors. RSC Adv 4:11197–11205
117. Liu M, Wang X, Huang Z, Guo P, Wang Z (2017) In-situ solution synthesis of graphene supported lamellar 1T-$MoTe_2$ for enhanced pseuducapacitors. Mater Lett 206:229–232
118. Ye T, Kuang Y, Xie C, Huang Z, Zhang C, Shan D, Zhou H (2014) Enhanced performance by polyaniline/tailored carbon nanotubes composite as supercapacitor electrode material. J Appl Polym Sci 131, Article number: 39971
119. Sekar P, Anothumakkoel B, Kurungot S (2015) 3D polyaniline porous layer anchored pillared graphene sheets: enhanced interface joined with high conductivity for better charge storage applications. ACS Appl Mater Interfaces 7:7661–7669
120. Chen L, Sun LJ, Luan F, Liang Y, Li Y, Liu XX (2010) Synthesis and pseudocapacitive studies of composite films of polyaniline and manganese oxide nanoparticles. J Power Sources 195:3742–3747
121. Rakhi RB, Chen W, Cha D, Alshareef HN (2012) Substrate dependent self-organization of mesoporous cobalt oxide nanowires with remarkable pseudocapacitance. Nano Lett 12:2559–2567
122. Chen Z, Augustyn V, Wen J, Zhang Y, Shen M, Dunn B, Lu Y (2011) High performance supercapacitors based on interwined CNT/V_2O_5 nanowire nanocomposites. Adv Mater 23:791–795
123. Wang YG, Li HQ, Xia YY (2006) Ordered whiskerlike polyaniline grown on the surface of mesoporous carbon and its electrochemical capacitance performance. Adv Mater 18:2619–2623
124. Hong SC, Kim S, Jong WJ, Jang WJ, Han TH, Hong JP, Oh JS, Hwang T, Lee Y, Lee JH, Nam JD (2004) Supercapacitor characteristics of pressurized RuO_2/carbon powder as binder-free electrodes. RSC Adv 4:48276–48284
125. Barbieri O, Hahn M, Foelske A, Kötz R (2006) Effect of electronic resistance and water content on the performance of RuO_2 for supercapacitors. J Electrochem Soc 153:A2049–A2054

126. Chaitra K, Sivaraman P, Vinny RT, Bhatta UM, Nagaraju N, Kathyayini N (2016) High energy density performance of hydrothermally produced hydrous ruthenium oxide/multiwalled carbon nanotubes composite: design of an asymmetric supercapacitor with excellent cycle life. J Energy Chem 25:627–635
127. Gnerlich M, Ben-Yoav H, Culver JN, Ketchum DR, Ghodssi R (2015) Selective deposition of nanostructured ruthenium oxide using Tobacco masaic virus for micro-supercapacitors in solid Nafion electrolyte. J Power Sources 293:649–656
128. Neupane S, Kaganas G, Valenzuela R, Kumari L, Wang XW, Li WZ (2011) Synthesis and characterization of ruthenium dioxide nanostructures. J Mater Sci 46:4803–4811
129. Lakshminarayana G, Kityk IV, Nagao T (2016) Synthesis, structural and electrical characterization of RuO_2 sol–gel spin-coating nano-films. J Mater Sci Mater Electron 27:10791–10797
130. Cho CJ, Noh MS, Lee WC, An CH, Kang CY, Hwang CS, Kim SK (2017) Ta-doped SnO_2 as a reduction-resistant oxide electrode for DRAM capacitors. J Mater Chem C 5:9405–9411
131. Hu CC, Chen WC (2004) Effects of substrates on the capacitive performance of RuOx center dot nH(2)O and activated carbon-RuOx electrodes for supercapacitors. Electrochim Acta 49:3469–3477
132. Hu CC, Chen WC, Chang KH (2004) How to achieve maximum utilization of hydrous ruthenium oxide for supercapacitors. J Electrochem Soc 151:A281–A290
133. Hu CC, Chang KH, Lin MC, Wu YT (2006) Design and tailoring of the nanotubular arrayed architecture of hydrous RuO_2 for next generation supercapacitors. Nano Lett 6:2690–2695
134. Chen MW (2013) Toward the theoretical capacitance of RuO_2 reinforced by highly conductive nanoporous Gold. Adv Energy Mater 3:851–856
135. Zhi M, Xiang C, Li J, Li M, Wu N (2013) Nanostructured carbon-metal oxide composite electrodes for supercapacitors: a review. Nanoscale 5:72–88
136. Faraji S, Ani FN (2015) The development supercapacitor from activated carbon by electroless plating—a review. Renew Sustain Energy Rev 42:823–834
137. Ramani M, Haran BS, White RE, Popov BN, Arsov L (2001) Studies on activated carbon capacitor materials loaded with different amounts of ruthenium oxide. J Power Sources 93:209–214
138. Yao Y, Yang Z, Sun H, Wang S (2012) Hydrothermal synthesis of Co_3O_4-graphene for heterogeneous activation of peroxymonosulfate for decomposition of phenol. Ind Eng Chem Res 51:14958–14965
139. Hu CC, Huang YH, Chang KH (2002) Annealing effects on the physicochemical characteristics of hydrous ruthenium and ruthenium-iridium oxides for electrochemical supercapacitors. J Power Sources 108:117–127
140. Wang Y, Guo J, Wang T, Shao J, Wang D, Yang YW (2015) Mesoporous transition metal oxides for supercapacitors. Nanomaterials 5:1667–1689
141. Arnold CB, Wartena RC, Swider-Lyons KE, Pigue A (2003) Direct-write planar microultracapacitors by laser engineering. J Electrochem Soc 150:A571–A575
142. Sopcic S, Rokovic MK, Mandic Z, Roka A, Inzelt G (2011) Mass changes accompanying the pseudocapacitance of hydrous RuO_2 under different experimental conditions. Electrochim Acta 56:3543–3548
143. Nquyen NL, Rochefort D (2014) Electrochemistry of ruthenium dioxide composite electrodes in diethylmethylammonium-triflate protic ionic liquid and its mixtures with acetonitrile. Electrochim Acta 147:96–103
144. Naveen AN, Selladurai S (2015) Fabrication and performance evaluation of symmetrical supercapacitor based on manganese oxide nanorods-PANI composite. Mater Sci Semicond Process 40:468–478
145. Warren R, Sammoura F, Tounsi F, Sanghadasa M, Lin LW (2015) Highly active ruthenium oxide coating via ALD and electrochemical activation in supercapacitor applications. J Mater Chem A 3:15568–15575
146. Zhan C, Lian C, Zhang Y, Thompson MW, Xie Y, Wu JZ, Kent PRC, Cummings PT, Jiang DE, Wesolowski DJ (2017) Computational insights into materials and interfaces for capacitive energy storage. Adv Sci 4, Article number: 1700059
147. Park PO, Lokhande CD, Park HS, Jung KD, Joo OS (2004) Performance of supercapacitor with electrodeposited ruthenium oxide film electrodes—effect of film thickness. J Power Sources 134:148–152
148. Ramani M, Haran BS, White RE, Popov BN, Arsov L (2001) Studies on activated carbon capacitor materials loaded with different amounts of ruthenium oxide. J Power Sources 93:209–214

149. Zubiao W, Shu T, Lili L, Yuping W (2012) Controlled particle size and shape of nanomaterials and their applications in supercapacitors in controlled nanofabrication. Pan Standford Publishing, Singapore, pp 473–519
150. Wang F, Xiao S, Hou Y, Hu C, Liu L, Wu Y (2013) Electrode materials for aqueous asymmetric supercapacitors. RSC Adv 3:13059–13084
151. Algharaibeh Z, Liu X, Pickup PG (2009) An asymmetric anthraquinone-modified carbon-ruthenium oxide supercapacitor. J Power Sources 187:640–643
152. Makino S, Yamauchi Y, Sugimoto W (2013) Synthesis of electro-deposited ordered mesoporous RuOx using lyotropic liquid crystal and application toward micro-supercapacitors. J Power Sources 227:153–160
153. Das B, Behm M, Lindbergh G, Reddy MV, Chowdari BVR (2015) High performance metal nitrides, MN (M = Cr, Co) nanoparticles for non-aqueous hybrid supercapacitors. Adv Powder Technol 26:783–788
154. Zhang C, Higgins TM, Park SH, O'Brien SE, Long D, Coleman JN, Nicolosi V (2016) Highly flexible and transparent solid-state supercapacitors based on RuO_2/PEDOT:PSS conductive ultrathin films. Nano Energy 28:495–505